JACS
JOURNAL OF THE AMERICAN CHEMICAL SOCIETY

COMMUNICATION

pubs.acs.org/JACS

The Use of NH_3 to Promote the Production of Large-Diameter Single-Walled Carbon Nanotubes with a Narrow (*n,m*) Distribution

Zhen Zhu, Hua Jiang,* Toma Susi, Albert G. Nasibulin, and Esko I. Kauppinen*

NanoMaterials Group, Department of Applied Physics and Center of New Materials, Aalto University, Puumiehenkuja 2, 00076 Aalto, Finland

Supporting Information

ABSTRACT: We demonstrate here a simple and effective (*n,m*)-selective growth of single-walled carbon nanotubes (SWCNTs) in an aerosol floating catalyst chemical vapor deposition (CVD) process by introducing a certain amount of ammonia (NH_3). Chiralities of carbon nanotubes produced in the presence of 500 ppm NH_3 at 880 °C are narrowly distributed around the major semiconducting (13,12) nanotube with over 90% of SWCNTs having large chiral angles in the range 20°−30°, and nearly 50% in the range 27°−29°. The developed synthesis process enables chiral-selective growth at high temperature for structurally stable carbon nanotubes with large diameters.

The electronic and optical properties of a single-walled carbon nanotube (SWCNT) depend on its chirality,[1] which is usually designated by a pair of integers (*n,m*) known as chiral indices, or equivalently identified by the tube diameter and its chiral angle. One cannot overemphasize the importance of establishing effective routes to facilitate the growth of carbon nanotubes with a preferred chiral structure. Over the past decade, substantial efforts have been devoted to developing various structure-controlled synthesis methods, of which most are based on the catalytic chemical vapor deposition (CVD) method, which is known to be an efficient and controllable process for carbon nanotube production.[2,3] A common practice to achieve high selectivity for SWCNT formation is to regulate the species, composition and size of the catalyst particles, typically in a bimetallic catalyst system such as CoMo(CAT),[4,5] FeRu,[6] FeCo,[7] NiFe,[8] and FeCu.[9] Although the growth mechanism remains veiled in mystery,[10] it is a fact that, in all reported works thus far, the resulting SWCNTs appear to exhibit very similar chirality distributions near the (6,5) nanotube, with most nanotubes having diameters below 1.0 nm and chiral angles close to 30°. A low growth temperature is usually required to achieve a narrow chirality distribution. An increase in the growth temperature is typically accompanied by an increase in the nanotube diameter as well as a broadening of the diameter distribution.[7] However, a low reaction temperature is usually adverse to high-yield growth of large-diameter SWCNTs, which are favored by certain applications[11] in high-performance electronics. In addition, we note that the chirality distribution in the above-mentioned chiral-selective SWCNT samples has so far been analyzed by optical spectrometry, mainly photoluminescence (PL), which is usually limited for a complete characterization in that only nanotubes with optical responses can be detected. Quantitative evaluation of the nanotube population is another issue since there is a lack of knowledge of the optical efficiency as a function of (*n,m*), not to mention the environmental effects.

In this communication, we report on the development of a new approach based on an aerosol floating-catalyst CVD process in order to promote the growth of SWCNTs with controlled chiral structure. By introducing a small amount of ammonia (NH_3) as an additive into the reaction, we succeeded in producing high-quality SWCNTs at a relatively high temperature, whose chiralities are largely clustered into a group around the (13,12) nanotube. The average tube diameter is 1.67 nm. Over 90% of SWCNTs were distributed in the high chiral angle region close to the armchair structure. Instead of optical measurements, structural characterization was carried out using electron diffraction technique which allows direct (*n,m*) measurements on individual SWCNTs. Electron diffraction analysis of SWCNT bundles endows us with further chiral angle distribution information. The measurements are free of nanotube environment effects.

SWCNTs were synthesized in a gas-phase floating catalyst CVD reactor[12] where iron nanoparticles derived from ferrocene vapor decomposition act as catalyst in a 400 cm^3/min flow of carbon monoxide (CO) and 2 cm^3/min of carbon dioxide (CO_2) at 880 °C. As an etching agent, small amounts of NH_3 were introduced into the reaction to amend the nanotube structure.[13] Three samples were obtained by regulating the amounts of NH_3 at 0 ppm, 500 ppm, and 1000 ppm, respectively, with all other parameters unchanged. All samples have been investigated by transmission electron microscopy (TEM) using a Philips CM200 FEG microscope and a JEOL-2200FS double aberration-corrected microscope, both being operated at 80 kV, which is well below the electron knock-on damage threshold for carbon.[14,15] The (*n,m*) determination from electron diffraction patterns (EDPs) of individual SWCNTs was based on a calibration-free intrinsic layer line-spacing method.[16] In addition, EDPs of SWCNT bundles provided supplementary knowledge on the chiral angle distributions in the samples.[17]

Electron microscopy observation showed that SWCNTs have been produced in the samples with NH_3 at 0 ppm as well as 500 ppm. Compared with that in the 0 ppm NH_3 sample, the yield of nanotubes is lower and the nanotubes are less bundled in the 500 ppm NH_3 sample. It is remarked that there are no carbon nanotubes observed in the sample synthesized with 1000 ppm NH_3. A representative TEM overview image of SWCNTs in the

Received: October 11, 2010
Published: December 30, 2010

dx.doi.org/10.1021/ja1087634 | *J. Am. Chem. Soc.* 2011, 133, 1224–1227

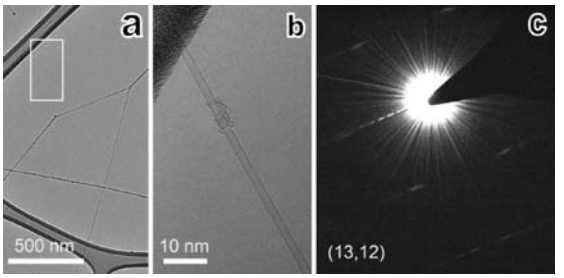

Figure 1. (a) Typical TEM overview image of SWCNTs produced in the presence of 500 ppm NH_3; (b) high-resolution TEM image of an individual SWCNT and (c) its corresponding EDP.

500 ppm NH_3 sample is presented in Figure 1a, where an individual nanotube is framed. Shown in Figure 1b and 1c are its high-resolution TEM image and the corresponding electron diffraction pattern (EDP), from which the chiral indices of the tube have been indexed as (13,12). More images and EDPs for the three investigated samples are available in the Supporting Information (**Figures S1−S3**). In general, the structure of the floating catalyst CVD nanotubes is well crystallized due to the high growth temperature. On the basis of electron diffraction analysis of 108 individual SWCNTs in the 500 ppm NH_3 sample, and 95 nanotubes in the 0 ppm NH_3 sample, we obtained (n,m) maps for both samples as shown in Figure 2. In the 500 ppm NH_3 sample, in total 37 different chiral structures were identified, of which the three main chiralities (13,12), (12,11), and (13,11) with abundances of 13, 8, and 8, respectively, constitute nearly 30% of the investigated nanotubes. In addition, the chiralities of the SWCNTs are seen intensively clustered into a narrow region around the major semiconducting (13,12) nanotube. In contrast, in the 0 ppm NH_3 sample, the chiralities are more broadly distributed. Out of 95 investigated nanotubes, a total number of 52 different ones are recognized in a different chiral configuration with (12,10) showing only a slightly higher abundance. We note that the fractions of semiconducting tubes in the above two samples, 65% for the non-NH_3 sample and 74% for the NH_3-enhanced sample, do not show substantial differences from each other nor from their inherent population of around 67%.

The prominence of the chirality distribution in the NH_3-enhanced sample is more effectively displayed in Figure 3 (red bars), which illustrates the ratio R_x/R_2 as a function of chiral angle. Here, R_x ($x = 1-3$) indicates the percentage of nanotubes with chiral angles in the ranges 0°−10°, 10°−20°, and 20°−30°, respectively. Our statistical data show that the 500 ppm NH_3 sample has more than 90% SWCNTs with large chiral angles in the range 20°−30°, and about 50% in the range 27°−29°. For the purpose of comparison, Figure 3 includes also the R_x/R_2 ratio for the 0 ppm NH_3 sample (blue bars), a CoMoCAT sample[5] (brown bars), and a hypothetical ratio calculated on the basis of the theoretical model proposed by Ding et al.[18] (green bars). It is apparent that the NH_3-enhanced sample stands out, giving an extremely high ratio of R_3/R_2, which demonstrates the high selectivity for growing SWCNTs with a narrow chirality distribution by introducing a certain amount of NH_3 into the CVD reaction. It is worth remarking that electron diffraction evaluation of SWCNT bundles leads to the same conclusion (Supporting Information, **Figure S4**).

Statistical analysis of the nanotube diameter distributions in the above two carbon nanotube samples are presented by the histograms in Figure 4 where red represents the 500 ppm NH_3 sample, and blue represents the 0 ppm NH_3 sample. In general, the nanotube diameters in both samples are similar, and close to those of conventional floating-catalyst-produced carbon nanotubes.[19] The average diameter is 1.60 nm for the 0 ppm NH_3 tubes and 1.67 nm, slightly increasing, for the 500 ppm NH_3 tubes. This implies that a small amount of NH_3 (up to 500 ppm) has little influence on the catalyst particle sizes, which are known to determine the nanotube diameters.[2,20] However, carbon nanotube growth was found to be terminated when 1000 ppm NH_3 was added into the reactor (Supporting Information, **Figure S3**).

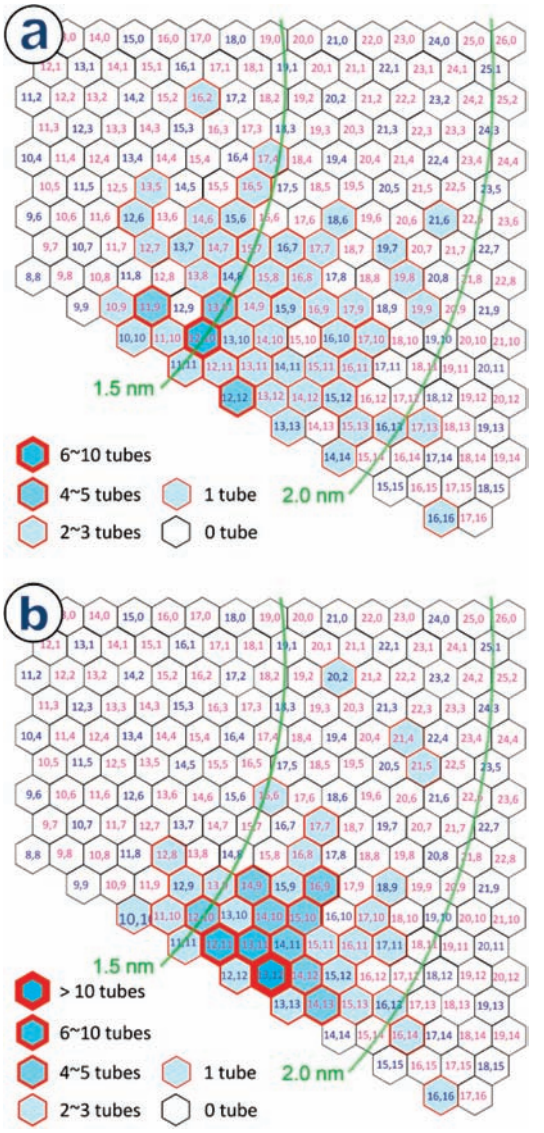

Figure 2. (n,m) maps for samples produced with (a) 0 ppm NH_3 and (b) 500 ppm NH_3.

It is an open question to discuss the role of NH_3 in growing SWCNTs with a narrow chirality distribution. On the basis of the existing experimental data, one reasonable explanation can be proposed that, as a strong etchant, NH_3 selectively etches off SWCNTs with small chiral angles, which are more reactive and less stable compared to high chiral angle tubes.[21] The same applies to nanotubes of smaller diameters due to their higher curvature,[22] which would explain the slightly enlarged average nanotube diameter as NH_3 is introduced. The NH_3 etching

dx.doi.org/10.1021/ja1087634 |J. Am. Chem. Soc. 2011, 133, 1224–1227

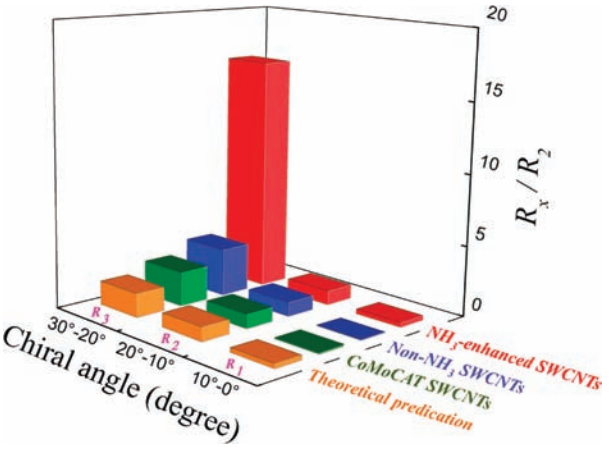

Figure 3. Chiral angle distribution in term of the ratio R_x/R_2 as a function of chiral angle. Here, R_x ($x = 1-3$) represents the percentage of nanotubes with chiral angles in the ranges 0°−10°, 10°−20°, and 20°−30°, respectively. The data for CoMoCAT sample come from ref 5, and the theoretical data from ref 18.

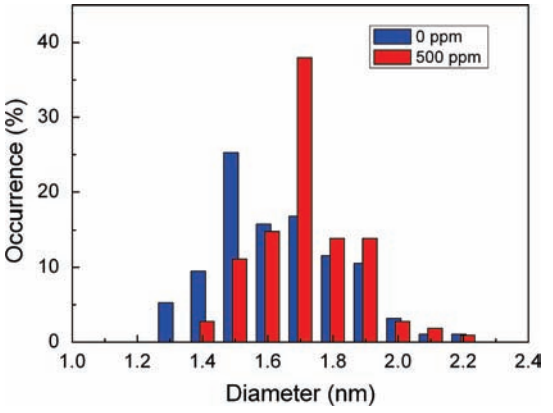

Figure 4. Histograms of SWCNT diameter distributions in samples of 0 ppm NH_3 (blue) and 500 ppm NH_3 (red).

action may take effect on the catalyst clusters already during nucleation, suppressing the growth of smaller chiral angle tubes that have a relatively larger number of dangling bonds on the growing edge of the hexagonal network. Those etching effects could explain the decreased yield and the reduced bundling of nanotubes observed with added NH_3. Apparently, such etching behavior would hardly lead to considerable electrical selectivity in the NH_3-enhanced sample.

Without doubt, the amount of NH_3 used in the reaction is a crucial factor. An excessive amount of NH_3 leads to a termination of the growth of carbon nanotubes. On the other hand, fine-tuning the NH_3 concentration could conceivably enhance chiral angle selectivity. Furthermore, recently it was reported that the diameters of carbon nanotubes can be effectively tuned in a similar floating catalyst CVD process by introducing controlled amounts of CO_2.[23] Therefore, we anticipate tunable selective growth of SWCNTs with preferred chiral structure by simultaneously regulating the amounts of NH_3 and CO_2 being introduced into the process.

To summarize, we succeeded in tailoring the (n,m) distribution of as-grown SWCNTs from an aerosol floating catalyst CVD process by introducing a certain amount of NH_3 as an etching agent. Unambiguous (n,m) determination of a number of individual SWCNTs based on electron diffraction analysis demonstrates that the chiral species of SWCNTs, produced in the presence of 500 ppm NH_3, cluster intensively into a narrow region around the major (13,12) nanotube. The mechanism for such selectivity is not certainly known at the moment, although we have preliminarily considered NH_3 etching effects as its origin. Further studies are in progress to address this issue. The developed synthesis process enables chiral-selective growth at high temperature for structurally stable carbon nanotubes with large diameters. This research opens up potential routes toward tunable (n,m) selective growth of single-walled carbon nanotubes.

■ ASSOCIATED CONTENT

Ⓢ Supporting Information. Figures S1−S4. This material is available free of charge via the Internet at http://pubs.acs.org.

■ AUTHOR INFORMATION

Corresponding Author
hua.jiang@tkk.fi; esko.kauppinen@tkk.fi

■ ACKNOWLEDGMENT

This work was jointly funded by the TEKES GROCO Project (No. 211072), the Academy of Finland (Project No. 128445), the CNB-E Project of the Aalto University MIDE research program, and by the European Commission under the FP6 STREP Project BNC Tubes (Contract NMP4-CT-2006-03350). Z.Z. is grateful to the Finnish National Graduate School in Materials Physics (NGSMP) for financial support.

■ REFERENCES

(1) Saito, R.; Dresselhaus, G.; Dresselhaus, M. S. *Physical Properties of Carbon Nanotubes*; Imperial College Press: London, 1998.
(2) Li, Y.; Kim, W.; Zhang, Y.; Rolandi, M.; Wang, D.; Dai, H. *J. Phys. Chem. B* **2001,** *105*, 11424–11431.
(3) Cheng, H. M.; Li, F.; Su, G.; Pan, H. Y.; He, L. L.; Sun, X.; Dresselhaus, M. S. *Appl. Phys. Lett.* **1998,** *72*, 3282–3284.
(4) Kitiyanan, B.; Alvarez, W. E.; Harwell, J. H.; Resasco, D. E. *Chem. Phys. Lett.* **2000,** *317*, 497–503.
(5) Bachilo, S. M.; Balzano, L.; Herrera, J. E.; Pompeo, F.; Resasco, D. E.; Weisman, R. B. *J. Am. Chem. Soc.* **2003,** *125*, 11186–11187.
(6) Li, X.; Tu, X.; Zaric, S.; Welsher, K.; Seo, W. S.; Zhao, W.; Dai, H. *J. Am. Chem. Soc.* **2007,** *129*, 15770–15771.
(7) Miyauchi, Y.; Chiashi, S.; Murakami, Y.; Hayashida, Y.; Maruyama, S. *Chem. Phys. Lett.* **2004,** *387*, 198–203.
(8) Chiang, W.-H.; Mohan Sankaran, R. *Nat. Mater.* **2009,** *8*, 882–886.
(9) He, M.; Chernov, A. I.; Fedotov, P. V.; Obraztsova, E. D.; Sainio, J.; Rikkinen, E.; Jiang, H.; Zhu, Z.; Tian, Y.; Kauppinen, E. I.; Niemelä, M.; Krause, A. O. I. *J. Am. Chem. Soc.* **2010,** *132* (40), 13994–13996.
(10) Wang, Q.; Ng, M.-F.; Yang, S.-W.; Yang, Y.; Chen, Y. *ACS Nano* **2010,** *4*, 939–946.
(11) Javey, A.; Guo, J.; Wang, Q.; Lundstrom, M.; Dai, H. *Nature* **2003,** *424*, 654–657.
(12) Moisala, A.; Nasibulin, A. G.; Brown, D. P.; Jiang, H.; Khriachtchev, L.; Kauppinen, E. I. *Chem. Eng. Sci.* **2006,** *61*, 4393–4402.
(13) Susi, T.; Nasibulin, A. G.; Ayala, P.; Tian, Y.; Zhu, Z.; Jiang, H.; Roquelet, C.; Garrot, D.; Lauret, J.-S.; Kauppinen, E. I. *Phys. Status Solidi B* **2009,** *246*, 2507–2510.
(14) Florian, B. *Rep. Prog. Phys.* **1999,** *62*, 1181.
(15) Krasheninnikov, A. V.; Banhart, F. *Nat. Mater.* **2007,** *6*, 723–733.

(16) Jiang, H.; Nasibulin, A. G.; Brown, D. P.; Kauppinen, E. I. *Carbon* **2007,** *45*, 662–667.
(17) Jiang, H.; Brown, D. P.; Nikolaev, P.; Nasibulin, A. G.; Kauppinen, E. I. *Appl. Phys. Lett.* **2008,** *93*, 141903.
(18) Ding, F.; Harutyunyan, A. R.; Yakobson, B. I. *Proc. Natl. Acad. Sci. U.S.A.* **2009,** *106*, 2506–2509.
(19) Tian, Y.; Jiang, H.; Pfaler, J. v.; Zhu, Z.; Nasibulin, A. G.; Nikitin, T.; Aitchison, B.; Khriachtchev, L.; Brown, D. P.; Kauppinen, E. I. *J. Phys. Chem. Lett.* **2010,** *1*, 1143–1148.
(20) Nasibulin, A. G.; Pikhitsa, P. V.; Jiang, H.; Kauppinen, E. I. *Carbon* **2005,** *43*, 2251–2257.
(21) Borstnik, U.; Hodoscek, M.; Janezic, D.; Lukovits, I. *Chem. Phys. Lett.* **2005,** *411*, 384–388.
(22) Gülseren, O.; Yildirim, T.; Ciraci, S. *Phys. Rev. B* **2002,** *65*, 153405.
(23) Tian, Y.; Zavodchikova, M.; Kivistö, S.; Nasibulin, A. G.; Zhu, Z.; Jiang, H.; Okhotnikov, O.; Kauppinen, E. I. K. Submitted to Small, 2010.